



Article

Affinity Maturation of a T-Cell Receptor-Like Antibody Specific for a Cytomegalovirus pp65-Derived Peptide Presented by HLA-A*02:01

Se-Young Lee ^{1,†}, Deok-Han Ko ^{1,†}, Min-Jeong Son ¹, Jeong-Ah Kim ¹, Keunok Jung ² and Yong-Sung Kim ^{1,2,*}

¹ Department of Molecular Science and Technology, Ajou University, Suwon 16499, Korea; sylee1117@ajou.ac.kr (S.-Y.L.); kdh701@ajou.ac.kr (D.-H.K.); minjeong96610@ajou.ac.kr (M.-J.S.); rhwjd319@ajou.ac.kr (J.-A.K.)

² Department of Allergy and Clinical Immunology, Ajou University School of Medicine, Suwon 16499, Korea; jung2767@ajou.ac.kr

* Correspondence: kimys@ajou.ac.kr; Tel.: +82-31-219-2662; Fax: +82-31-219-1610

† These authors have contributed equally to this work.

Abstract: Human cytomegalovirus (CMV) infection is widespread among adults (60–90%) and is usually undetected in healthy individuals without symptoms but can cause severe diseases in immunocompromised hosts. T-cell receptor (TCR)-like antibodies (Abs), which recognize complex antigens (peptide–MHC complex, pMHC) composed of MHC molecules with embedded short peptides derived from intracellular proteins, including pathogenic viral proteins, can serve as diagnostic and/or therapeutic agents. In this study, we aimed to engineer a TCR-like Ab specific for pMHC comprising a CMV pp65 protein-derived peptide (⁴⁹⁵NLVPMVATV⁵⁰³; hereafter, CMVpp65₄₉₅₋₅₀₃) in complex with MHC-I molecule human leukocyte antigen (HLA)-A*02:01 (CMVpp65₄₉₅₋₅₀₃/HLA-A*02:01) to increase affinity by sequential mutagenesis of complementarity-determining regions using yeast surface display technology. Compared with the parental Ab, the final generated Ab (C1-17) showed ~67-fold enhanced binding affinity ($K_D \approx 5.2$ nM) for the soluble pMHC, thereby detecting the cell surface-displayed CMVpp65₄₉₅₋₅₀₃/HLA-A*02:01 complex with high sensitivity and exquisite specificity. Thus, the new high-affinity TCR-like Ab may be used for the detection and treatment of CMV infection.

Keywords: cytomegalovirus; peptide/major histocompatibility complex class I complex; T-cell-receptor-like antibody; affinity maturation; yeast surface display



Citation: Lee, S.-Y.; Ko, D.-H.; Son, M.-J.; Kim, J.-A.; Jung, K.; Kim, Y.-S. Affinity Maturation of a T-Cell Receptor-Like Antibody Specific for a Cytomegalovirus pp65-Derived Peptide Presented by HLA-A*02:01. *Int. J. Mol. Sci.* **2021**, *22*, 2349. <https://doi.org/10.3390/ijms22052349>

Academic Editor: Yong-Seok Heo

Received: 1 February 2021

Accepted: 23 February 2021

Published: 26 February 2021

Publisher's Note: MDPI stays neutral with regard to jurisdictional claims in published maps and institutional affiliations.



Copyright: © 2021 by the authors. Licensee MDPI, Basel, Switzerland. This article is an open access article distributed under the terms and conditions of the Creative Commons Attribution (CC BY) license (<https://creativecommons.org/licenses/by/4.0/>).

1. Introduction

Human cytomegalovirus (CMV), a β -herpes virus with a double-stranded DNA, infects a wide variety of cells and establishes latency in the host [1]. CMV infection is very common in adults (60–90% of the population), with higher infection rates with age [2], and is usually asymptomatic in healthy subjects but can cause severe diseases in immunocompromised patients with cellular immunosuppression or immunodeficiency, including transplant recipients and fetuses [1,3].

Major histocompatibility complex class I (MHC-I) molecules, also known as human leukocyte antigen I (HLA-I), are cell-surface antigen-presenting proteins displaying peptide fragments (8–10 amino acid residues in length) derived from intracellular cytoplasmic proteins, including self, viral, and tumor antigens, for recognition by CD8⁺ T cells [4]. In CMV-seropositive hosts, matrix protein pp65 is among the most frequently immunologically recognized CMV antigens [5], accounting for 70–90% of the cytotoxic CD8⁺ T cells' (CTLs) response to CMV [6]. Among the pp65-derived CTL epitope peptides, the 9-mer peptide ⁴⁹⁵NLVPMVATV⁵⁰³ (residues 495–503; hereafter referred to as CMVpp65₄₉₅₋₅₀₃ peptide) is the most immunogenic T cell epitope predominantly displayed on HLA-A*02:01, the most common MHC-I allele in the population [6–8]. Hence, detection and targeting of the

highly prevalent CMVpp65₄₉₅₋₅₀₃/HLA-A*02:01 complex on the surface of CMV-infected cells are crucial for the development of detection and/or therapeutic modalities [9,10]. T-cell receptors (TCRs) specifically recognize the peptide–MHC complex (pMHC), but their natural affinity is limited to ~1–100 μ M [4]. Alternatively, antibodies (Abs) called TCR-like Abs can be engineered to specifically recognize pMHC with high affinity [9,11].

A number of TCR-like Abs directed toward a particular pMHC derived from a pathogenic viral protein or a tumor-associated antigen have been developed because such Abs have many desirable features of conventional immunoglobulin G (IgG) Abs, including large-scale manufacturing capacity and long serum half-life [11]. However, few of these Abs have reached clinical application, and the optimal specificity and affinity of TCR-like Abs need to be defined. High-affinity TCR-like Abs have several potential biomedical applications and may be valuable research reagents for detecting specific virus-/tumor-associated pMHCs on cell and tissue surfaces [11,12].

Previously, a TCR-like Ab (H9) specific for the CMVpp65₄₉₅₋₅₀₃/HLA-A*02:01 complex was reported [13]. However, the affinity was relatively weak ($K_D = 300$ nM), limiting its potential use as a detection or therapeutic reagent. Here, we aimed to engineer H9 to increase its affinity by ~67-fold for pMHC comprising the CMVpp65₄₉₅₋₅₀₃/HLA-A*02:01 complex by yeast surface display (YSD) technology, thereby enabling highly sensitive and specific detection of the cell surface-displayed pMHC.

2. Results

2.1. Evaluation of Parental H9

The TCR-like H9 antigen-binding fragment (Fab) was previously isolated by screening a large phage-displayed human Fab library against a recombinant CMVpp65₄₉₅₋₅₀₃/HLA-A*02:01 complex [13]. H9 reformatted into the bivalent IgG form showed binding specificity to soluble pMHC comprising the CMVpp65₄₉₅₋₅₀₃/HLA-A*02:01 complex with relatively weak binding affinity ($K_D \approx 300$ nM) [13]. Here, we generated H9 in the mouse IgG2a/ κ format and evaluated its binding activity by flow cytometry toward the cell surface-displayed CMVpp65₄₉₅₋₅₀₃/HLA-A*02:01 complex, generated by external peptide pulsing of cells expressing HLA-A*02:01 at various levels (Figure 1A). Even at 500 nM, H9 manifested very weak binding activity only toward MDA-MB-231 and Malme-3M cells expressing HLA-A*02:01 at relatively high levels (HLA-A*02:01⁺⁺) but negligible or little binding activity toward HCT116 cells expressing HLA-A*02:01 at moderate levels (HLA-A*02:01⁺) and toward HLA-A*02:01-negative LoVo cells (Figure 1B). At 100 and 20 nM, H9 binding to peptide-loaded HLA-A*02:01⁺⁺ MDA-MB-231 cells was negligible (Figure 1C). H9 did not react with cells loaded with an off-target peptide of HLA-A*02:01-restricted human papilloma virus (HPV) type 16 E7 protein-derived 9-mer peptide, HPV E7₁₁₋₁₉ (¹¹YMLDLQPETV¹⁹). These results confirmed the specific binding of H9 to the membrane-bound pMHC comprising the CMVpp65₄₉₅₋₅₀₃/HLA-A*02:01 complex.

However, the binding strength was too weak to detect the complex on cells expressing HLA-A*02:01 at moderate levels. Thus, we sought to engineer H9 for affinity improvement.

2.2. Affinity Maturation of H9 to Generate C1 Ab

Owing to lack of information regarding specific amino acid residue interactions between H9 and the CMVpp65₄₉₅₋₅₀₃/HLA-A*02:01 complex, for affinity maturation, we first generated an H9 library by randomization of the third complementarity-determining region (CDR) of variable regions of the heavy chain (VH) and (VL), i.e., VH-CDR3 and VL-CDR3, known to be major contributors to Ab–antigen interaction [14]. Most residues in VH-CDR3 (residues 95–102 in Kabat numbering [15]) and VL-CDR3 (residues 89–97) were randomized with degenerate codons, including the NNK codon encoding all 20 amino acids and one stop codon (Figure 2A). To improve the stability and folding efficiency of the Ab, some highly conserved amino acid residues based on human germline sequences, inferred from the International ImMunoGeneTics information system database [16], were conserved or minimally randomized to maintain the parental amino acid residues at a

high frequency. Specifically, in the last three residues of VH-CDR3 (100J, 101, and 102), which are highly conserved with a consensus sequence of 100J_{Phe}/Met/Ile–Asp–Tyr₁₀₂, only the PheH100J residue was randomized with the degenerate codon WTK (encoding F, I, M, and L) while preserving the other residues, AspH101 and TyrH102. Similarly, for VL-CDR3, the highly conserved residues GlnL89, ProL95, and ThrL97 were retained owing to their high frequency in the human germline sequences. Residues TyrL91, SerL94, and PheL96 were mutated with degenerate codons YHT (encoding F, S, Y, L, P, and H), WHT (encoding F, S, Y, I, T, and N), NNT (encoding F, S, Y, C, L, P, H, R, I, T, N, S, V, A, D, and G), respectively (Figure 2A). The VH-CDR3/VL-CDR3-randomized H9 library was generated by YSD technology in the single-chain Fab (scFab) format, wherein the C-terminus of VL was linked to the N-terminus of VH via a G4S-based 63-amino-acid linker (Figure 2A) [17,18]. The library diversity was $\sim 1.5 \times 10^7$, and sequencing of tens of clones confirmed the fidelity of the library diversity.

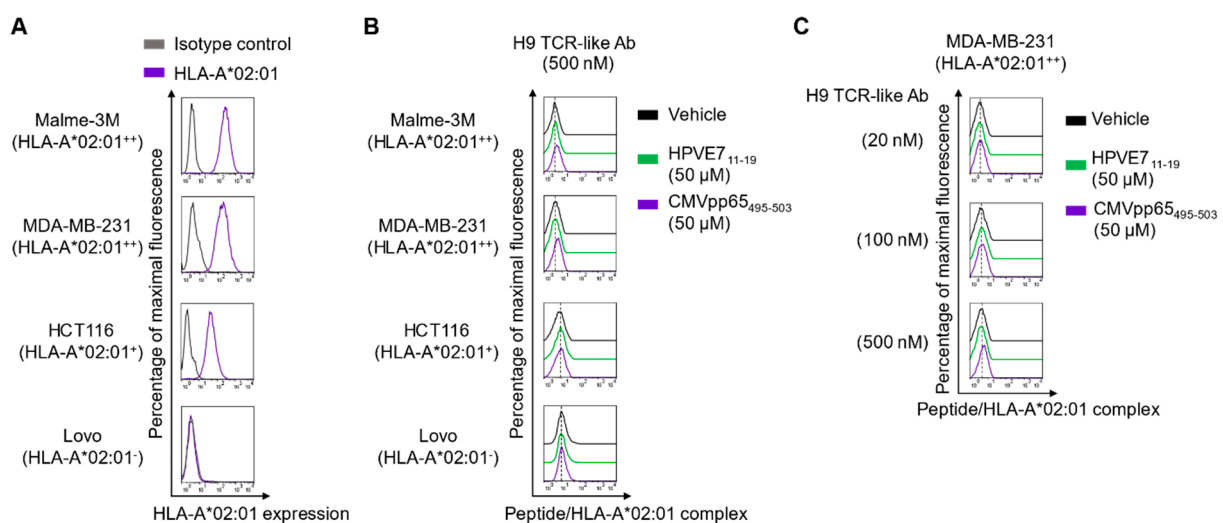


Figure 1. Evaluation of H9 binding to the cell surface-displayed CMVpp65₄₉₅₋₅₀₃/HLA-A*02:01 complex. (A) Flow cytometric analysis of the cell surface expression levels of human leukocyte antigen (HLA)-A*02:01, classified as ++ (high level) for both MDA-MB-231 and Malme-3M cells, as + (positive) for HCT116 cells, and as - (negative) for LoVo cells. (B,C) Flow cytometric analysis of H9 binding at 500 nM (B) to peptide-pulsed cells (B) and at various concentrations to peptide-pulsed MDA-MB-231 cells (C). Cells were pulsed with the vehicle, CMVpp65₄₉₅₋₅₀₃ peptide (50 μM), or the control HLA-A*02:01-restricted HPVE7₁₁₋₁₉ (50 μM) peptide for 3 h at 37 °C and incubated with H9 and then the Alexa Fluor 647-conjugated goat anti-mouse immunoglobulin G (IgG)-specific (Fab')₂ antibody (Ab) (secondary Ab) prior to flow cytometry. In (A–C), representative histograms from two independent experiments are depicted.

Table 1. Parameters of binding kinetics of TCR-like Abs in relation to the CMVpp65₄₉₅₋₅₀₃/HLA-A*02:01 SCT protein, as measured using biolayer interferometry.

Abs	K _D (nM)	k _{on} (M ⁻¹ s ⁻¹)	k _{off} (s ⁻¹)	R ²
H9	348 ± 33	(6.3 ± 3.3) × 10 ³	(2.2 ± 0.2) × 10 ⁻³	0.97
C1	12.6 ± 0.3	(1.8 ± 0.2) × 10 ⁵	(2.3 ± 0.4) × 10 ⁻³	0.97
C38	30.6 ± 0.1	(1.5 ± 0.1) × 10 ⁵	(4.7 ± 0.4) × 10 ⁻³	0.98
C1-17	5.2 ± 0.1	(9.3 ± 0.2) × 10 ⁵	(4.8 ± 0.1) × 10 ⁻³	0.99
C1-30	8.7 ± 0.1	(8.0 ± 0.2) × 10 ⁵	(7.0 ± 0.1) × 10 ⁻³	0.99

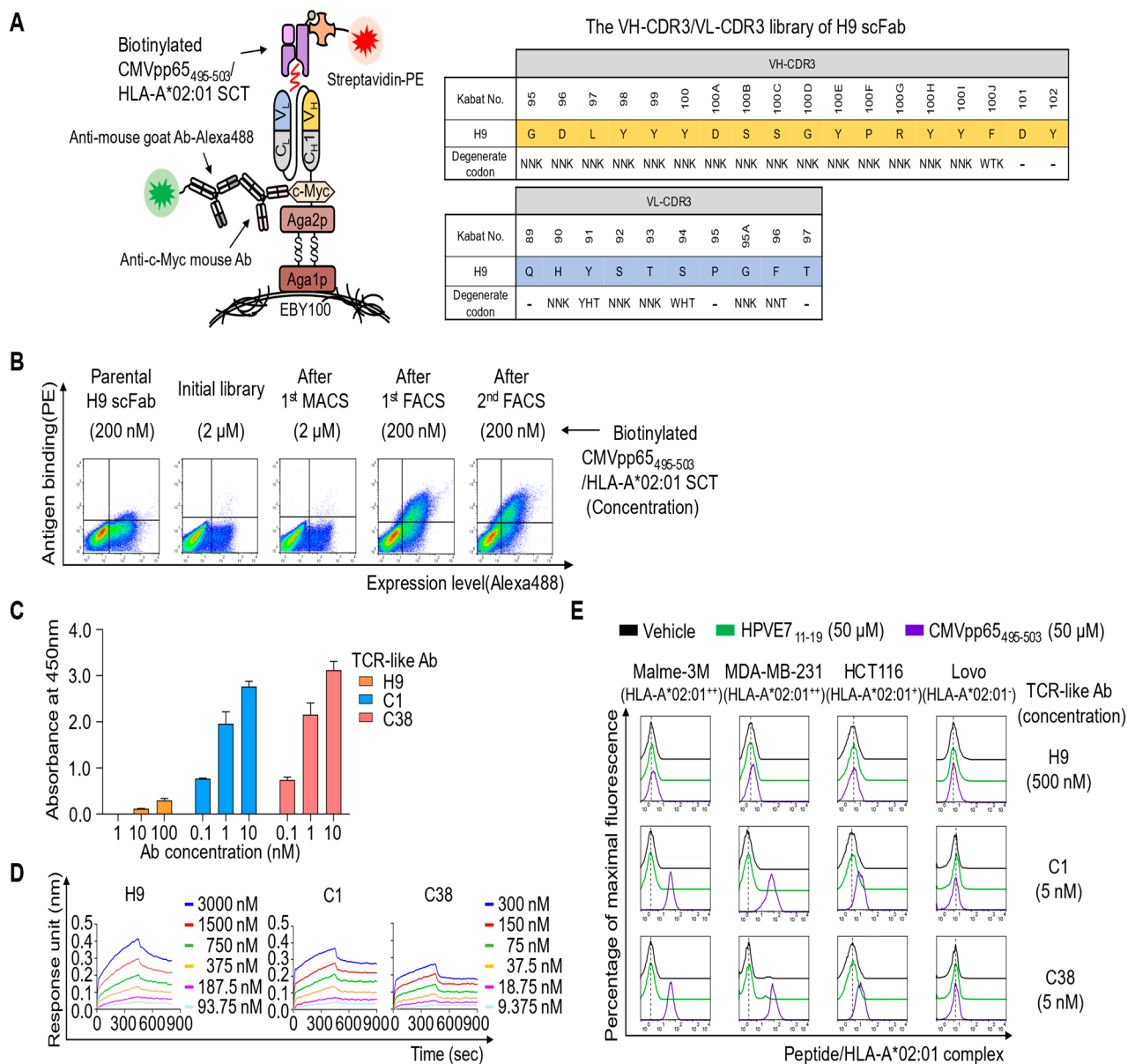


Figure 2. Affinity maturation of H9 and characterization of the isolated clones. **(A)** The scheme of library construction and screening for H9 in the single-chain antigen-binding fragment (scFab) format using YSD technology. The indicated residues in VH-CDR3 and VL-CDR3 were randomized with the indicated degenerate codons. The “-” sign denotes conserved residues. **(B)** Flow cytometric analysis of antigen binding and expression levels of the yeast surface-displayed scFab library pool enriched after each round of screening by magnetically activated cell sorting (MACS) and fluorescence-activated cell sorting (FACS), compared with those of the parental H9 scFab. **(C)** Dose-dependent binding activity of the isolated and purified Abs in mouse IgG2a/κ form toward the microtiter plate coated with peptide–MHC complex (pMHC) comprising CMVpp65₄₉₅₋₅₀₃/HLA-A*02:01 single-chain trimer (SCT) antigen, as determined by ELISA. **(D)** Binding isotherms of the immobilized Abs toward the soluble CMVpp65₄₉₅₋₅₀₃/HLA-A*02:01 SCT antigen, as measured by biolayer interferometry. pMHC concentrations are indicated (colored). The kinetic interaction parameters are listed in Table 1. **(E)** Flow cytometric analysis of the binding of the isolated T-cell receptor (TCR)-like Abs at the indicated concentrations to the peptide-pulsed cells. Peptide pulsing and flow cytometric analysis were performed as described in Figure 1C. Representative histograms from two independent experiments are depicted.

For library screening, we prepared the soluble antigen of CMVpp65₄₉₅₋₅₀₃/HLA-A*02:01 single-chain trimer (SCT) protein with a C-terminal Avi tag (for biotinylation) (Supplementary Figure S1). We engineered the SCT form to have an artificial disulfide bridge between the HLA α1 domain (Tyr108Cys) and linker L1 (position 2 of L1) to maintain

stable binding of CMVpp65₄₉₅₋₅₀₃ into the groove of the MHC-I complex (Supplementary Figure S1) [19,20]. The disulfide-bonded SCT format ensured that the TCR-like Ab does not recognize MHC-I alone. As an off-target antigen, the HPVE7₁₁₋₁₉/HLA-A*02:01 SCT protein was prepared similarly. The pMHC SCT proteins were expressed in cultured HEK293F cells. The purified protein (~49.7 kDa) was site-specifically biotinylated, as confirmed by a streptavidin gel shift assay (Supplementary Figure S1C).

The H9 library was screened by one round of magnetically activated cell sorting (MACS), followed by two rounds of fluorescence-activated cell sorting (FACS) with the biotinylated CMVpp65₄₉₅₋₅₀₃/HLA-A*02:01 SCT antigen in the presence of a 10-fold higher concentration of the non-biotinylated off-target HPVE7₁₁₋₁₉/HLA-A*02:01 SCT antigen (Figure 2B), thereby yielding two unique good-affinity binders, C1 and C38 scFabs (Supplementary Figure S2). The isolated scFab clones were converted into the mouse IgG2a/ κ form and expressed in HEK293F cells. ELISA revealed that purified C1 and C38 bound to the soluble CMVpp65₄₉₅₋₅₀₃/HLA-A*02:01 SCT in proportion to the concentration, thus showing much stronger binding activity than parental H9 (Figure 2C). In a kinetic binding analysis performed by biolayer interferometry, Abs C1 and C38 manifested more than 10-fold stronger affinity ($K_D \approx 13$ and 31 nM, respectively) than that of parental H9 ($K_D \approx 348$ nM; Figure 2D and Table 1). The binding specificity of the affinity-matured TCR-like Abs to the cell surface-displayed CMVpp65₄₉₅₋₅₀₃/HLA-A*02:01 complex was evaluated by flow cytometry using cells pulsed with peptides. Compared with parental H9 at 500 nM, both C1 and C38, even at a 100-fold lower concentration (at 5 nM), exhibited a substantial binding activity toward HLA-A*02:01-positive cells, including HLA-A*02:01⁺ HCT116 cells (Figure 2E). However, the affinity-matured Abs did not bind at all to the same HLA-A*02:01-positive cells loaded with the off-target HPVE7₁₁₋₁₉ peptide or to HLA-A*02:01-negative LoVo cells (Figure 2E), thereby confirming their binding specificity to the cell surface-displayed CMVpp65₄₉₅₋₅₀₃/HLA-A*02:01 complex. Thus, both Abs C1 and C38 may exhibit improved affinity while maintaining their specificity.

The association rate constant (k_{on}), dissociation rate constant (k_{off}), and equilibrium dissociation constant (K_D) and an estimate of the goodness of curve fit (R^2) were calculated in the Octet Data Analysis software, v.11.0 (ForteBio).

2.3. Affinity Maturation of C1 to Generate High-Affinity TCR-Like Abs

Considering the very low density of specific peptide/HLA complexes on a natural cell surface (≤ 1000 per cell [21]), successful therapeutic and detection use of a TCR-like Ab requires strong affinity and high specificity [22]. Therefore, we selected C1, which has higher affinity than C38, for the next round of affinity maturation. For affinity maturation of C1, the VH-CDR2 (residues 50–65) and VL-CDR2 (residues 50–56) regions (except for the residues generally conserved in human germline sequences, e.g., IleH51, TyrH59, and AlaH60 in VH-CDR2 and AlaL51 and SerL52 in VL-CDR2) were randomized using degenerate codons (Figure 3A). The library was generated in the scFab format by YSD technology with a diversity of $\sim 1.3 \times 10^7$ and was screened by four rounds of FACS against the biotinylated antigen, CMVpp65₄₉₅₋₅₀₃/HLA-A*02:01 SCT, with a gradual decrease in antigen concentration in the presence of a 10-fold higher concentration of the non-biotinylated off-target competitor, HPVE7₁₁₋₁₉/HLA-A*02:01 SCT (Figure 3B,C). Analysis of more than 50 finally isolated clones yielded two unique clones, C1-17 and C1-30 (Supplementary Figure S2). The isolated clones were reformatted into mouse IgG2a/ κ form and purified for further characterization. ELISA indicated improved binding activity of both C1-17 and C1-30 for the soluble CMVpp65₄₉₅₋₅₀₃/HLA-A*02:01 SCT compared with C1 (Figure 3D). Binding kinetics analysis revealed that C1-17 and C1-30 showed single-digit nanomolar affinities (K_D) of ~ 5.2 and ~ 8.7 nM, respectively, which were approximately twofold stronger than that of parental C1 ($K_D \approx 13$ nM; Table 1). In all cases, affinity improvement was essentially owing to an increase in the association rate constant k_{on} (Figure 3E and Table 1).

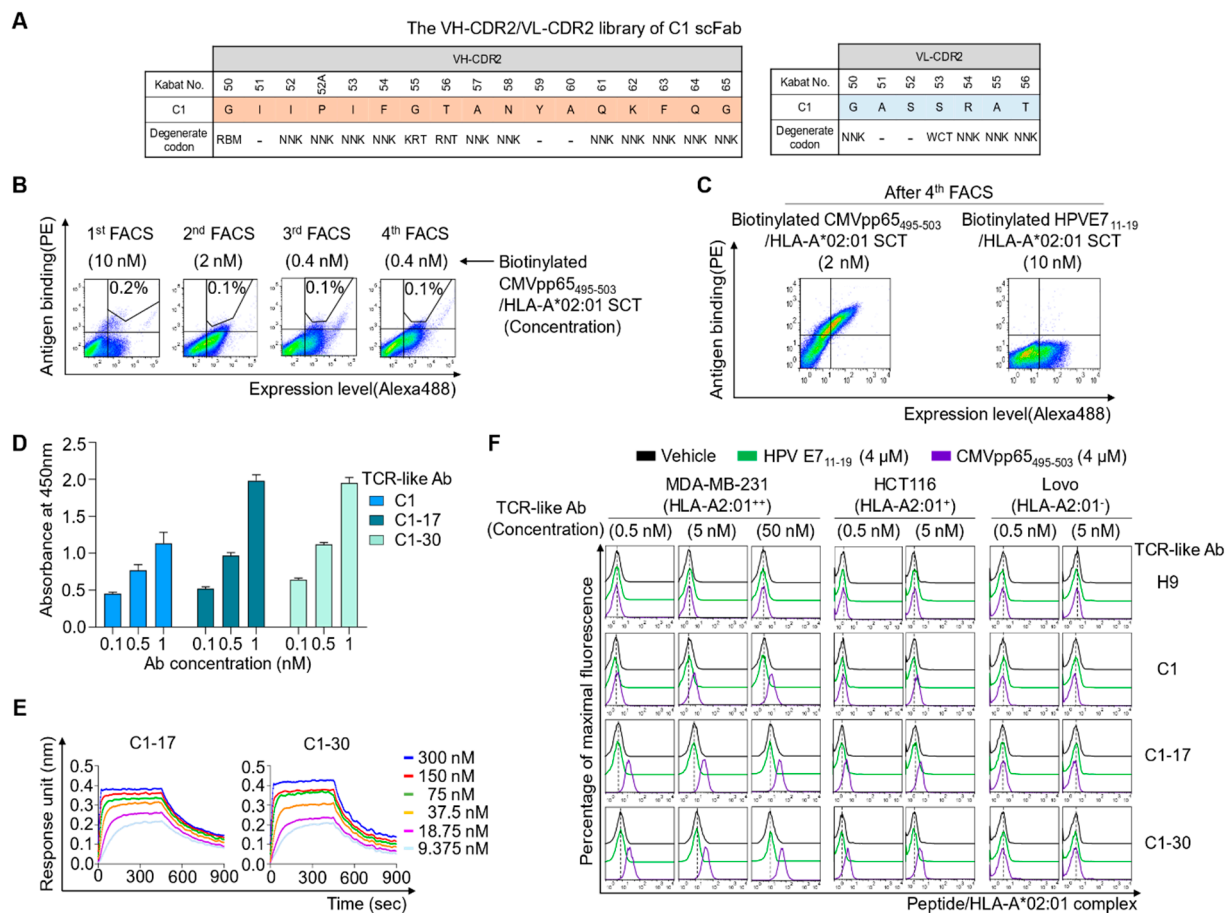


Figure 3. Affinity maturation of C1 Ab to generate high-affinity TCR-like Abs. **(A)** The scheme of yeast scFab library construction for VH-CDR2 and VL-CDR2 of C1 Ab, wherein the indicated residues were randomized with the indicated degenerate codons. The “-” sign indicates conserved residues. **(B)** Flow cytometric sorting gate plots of the yeast surface-displayed scFab library screening in each round of screening by FACS with the indicated concentration of the biotinylated CMVpp65₄₉₅₋₅₀₃/HLA-A*02:01 SCT antigen in the presence of a 10-fold higher concentration of the non-biotinylated off-target HPVE7₁₁₋₁₉/HLA-A*02:01 SCT protein. **(C)** Flow cytometric analysis of target-specific enrichment for the yeast surface-displayed scFab library pool enriched after four rounds of FACS using the indicated target and off-target antigen. **(D)** Dose-dependent binding activity of the isolated and purified Abs in mouse IgG2a/ κ form toward the microtiter plate coated with pMHC comprising CMVpp65₄₉₅₋₅₀₃/HLA-A*02:01 complex antigen, as determined by ELISA. **(E)** Binding isotherms of the immobilized IgG2a/ κ Abs toward the soluble CMVpp65₄₉₅₋₅₀₃/HLA-A*02:01 complex antigen, as measured by biolayer interferometry. The concentrations of pMHC are indicated (colored). The kinetic interaction parameters are listed in Table 1. **(F)** Flow cytometric analysis of binding of the TCR-like Abs in IgG2a/ κ form at the indicated concentrations to peptide-pulsed cells. Cells were pulsed for 3 h at 37 °C with the vehicle, CMVpp65₄₉₅₋₅₀₃ peptide (4 μ M), or the control, HLA-A*02:01-restricted HPVE7₁₁₋₁₉ (4 μ M) peptide, and incubated with the TCR-like Abs at the indicated concentrations and then with the Alexa Fluor 647-conjugated goat anti-mouse IgG-specific (Fab')₂ Ab (secondary Ab) prior to flow cytometry. Representative histograms from two independent experiments are depicted.

Next, we assessed the specificity and lower detection limits of the affinity-matured Abs toward cells pulsed with the peptide at a low concentration (down to 4 μ M) to generate low-density CMVpp65₄₉₅₋₅₀₃/HLA-A*02:01 complex on cells. Both C1-17 and C1-30 strongly stained HLA-A*02:01-positive cells loaded with CMVpp65₄₉₅₋₅₀₃ in proportion to the concentration but did not stain the same cells pulsed with a vehicle or the off-target HPVE7₁₁₋₁₉ peptide and HLA-A*02:01-negative cells (Figure 3F). Although parental C1 at a low concentration of 0.5 nM failed to detect the membrane-bound CMVpp65₄₉₅₋₅₀₃/HLA-A*02:01 complex, both C1-17 and C1-30 at the same concentration detected it (Figure 3F). Thus,

affinity-matured TCR-like Abs C1-17 and C1-30 reliably detected the cell surface-displayed CMVpp65₄₉₅₋₅₀₃/HLA-A*02:01 complex with high sensitivity and exquisite specificity.

3. Discussion

The low affinity of TCR-like Abs is one of the major hurdles associated with their detection and therapeutic applications. We engineered a TCR-like Ab H9 specific for the CMVpp65₄₉₅₋₅₀₃/HLA-A*02:01 complex to improve H9's affinity while retaining its specificity. We performed two rounds of affinity maturation by sequential random mutagenesis on the VH-/VL-CDR3 of H9 and then on the VH-/VL-CDR2 of C1 in the scFab format using YSD technology. The finally generated, highest-affinity Ab C1-17 possessed ~67-fold improved affinity ($K_D \approx 5.2$ nM) compared with that of the parental H9 ($K_D \approx 348$ nM). Parental H9 failed to detect the membrane-bound CMVpp65₄₉₅₋₅₀₃/HLA-A*02:01 complex even on HLA-A*02:01⁺ cells at a concentration below 500 nM. Conversely, both C1-17 and C1-30 with single-digit nanomolar affinities detected the cell surface-displayed CMVpp65₄₉₅₋₅₀₃/HLA-A*02:01 complex at a 1000-fold lower concentration (0.5 nM) even on HLA-A*02:01⁺ HCT116 cells, thereby showing high sensitivity owing to affinity maturation. They did not bind to HLA-A*02:01-positive cells, unpulsed or pulsed with an off-target peptide, nor to HLA-A*02:01-negative cells, thus confirming their exquisite specificity.

The expression levels of the pMHC complex on the cell surface are relatively low, ranging from tens to hundreds of molecules/cell, compared with other membrane receptors [11]. For example, the CMVpp65₄₉₅₋₅₀₃/HLA-A*02:01 complex was reported to be ~100 molecules/cell on the surface of CMV-infected fibroblasts [13]. Accordingly, TCRs or TCR-like Abs with high affinity and specificity are necessary for the sensitive detection or targeting of the low copy numbers of pMHC [10,11,22]. Though the H9 Ab detected the CMVpp65₄₉₅₋₅₀₃/HLA-A*02:01 on the surface of CMV-infected fibroblasts [13], it has not been further developed. The high-affinity TCR-like C1-17 Ab, engineered to have a $K_D \approx 5.2$ nM in this study, can be developed as a research agent to detect CMVpp65₄₉₅₋₅₀₃/HLA-A*02:01 presentation on the surface of and inside cells during CMV infection and as a therapeutic agent to eliminate CMV-infected cells.

The full-length TCR-like Ab was generated based on the Fc portion of mouse IgG2a rather than that of human IgG isotype for use as a detection agent for the CMVpp65₄₉₅₋₅₀₃/HLA-A*02:01 complex on human cells and tissues. The mouse IgG2a isotype also has merits as a primary Ab in detection because it exhibits a detection sensitivity with labeled anti-mouse IgG isotype-specific secondary Abs that is superior to that of the other mouse IgG isotype Abs [23], and the anti-mouse IgG2a-specific secondary Abs are readily available. To be used as a therapeutic Ab, the constant regions of the TCR-like Ab need to be switched into human IgG1 with greater effector functions than the other isotypes [24].

A few antiviral drugs, including ganciclovir and valganciclovir, have been used for treating CMV infection, but viral resistance is a major challenge associated with their use [1]. Another approach is the transfer of donor-derived CMV-specific CTLs, but it remains limited due to the occurrence of graft-versus-host disease (GVHD) in allogeneic recipients [25]. The high-affinity TCR-like Ab C1-17 can be converted into a bispecific T-cell engager [20] and a chimeric antigen receptor (CAR) for CAR-T therapy based on the autologous T-cells to overcome allogeneic immunogenicity [3,26]. Moreover, C1-17 can be developed as a therapeutic Ab to eliminate CMV-infected cells through the effector functions, such as Ab-dependent cellular cytotoxicity [27,28], or via a targeting agent to deliver cytotoxic payloads, such as potent drugs and toxins [9,29]. Comparative analyses of CTL responses in CMV-seropositive individuals have shown that, among the CMV-derived CTL epitopes, the pp65-derived CMVpp65₄₉₅₋₅₀₃ and the major immediate-early gene product (IE-1)-derived VLEETSVML peptide (residues 316–324) are the most frequent CTL epitope peptides, with the former being more dominant than the latter [5,6,30]. CMVpp65₄₉₅₋₅₀₃ is predominantly presented by HLA-A*02:01, one of the most frequent MHC-I alleles in the human population (30~50%, depending on the ethnicity) [27]. Accordingly, C1-17 specific for the CMVpp65₄₉₅₋₅₀₃/HLA-A*02:01 complex could be used in a maximum of up to

~50% of CMV-infected individuals as a detection or therapeutic agent. Nonetheless, C1-17, restricted to the single HLA-A*02:01 allele, is not suitable for broad applicability due to the three HLA genes and their thousands of polymorphic alleles in humans [9].

This study has some limitations. The engineered TCR-like Abs specific for CMVpp65₄₉₅₋₅₀₃-bound HLA-A*02:01 were evaluated only for cells exogenously pulsed with peptides. Thus, the high-affinity TCR-like C1-17 Ab must be further validated as a potential detection and/or therapeutic agent for the pMHC naturally presented on CMV-infected cells, such as fibroblasts, epithelial cells, endothelial cells, neurons, monocytes, and macrophages, which are susceptible to CMV infection [31–33], in comparison with the lower-affinity clones, including the parent H9 Ab [13].

In conclusion, we developed a high-affinity TCR-like Ab (C1-17) specific for the highly prevalent pMHC of CMV infection, i.e., the CMVpp65₄₉₅₋₅₀₃/HLA-A*02:01 complex, in both soluble and membrane-bound forms. In addition to its value as a study reagent, the high-affinity TCR-like Ab can be utilized as a therapeutic agent against CMV infection.

4. Materials and Methods

4.1. Peptides and Plasmids

Human CMV pp65-derived 9-mer peptide, CMVpp65₄₉₅₋₅₀₃ (⁴⁹⁵NLVPMVATV⁵⁰³), and human papilloma virus (HPV) type 16 E7 protein-derived 9-mer peptide, HPVE7₁₁₋₁₉ (¹¹YMLDLQPETV¹⁹), were synthesized with 95% purity (AnyGen, Gwangju, Korea). DNA fragments encoding the variable regions of the heavy chain (VH) and light chain (VL) of H9 (patent US8361473B2) were synthesized (Bioneer, Daejeon, Korea), and respective VH and VL genes were subcloned into a modified pcDNA 3.4 VH vector (Invitrogen, CA, USA) carrying the mouse IgG2a constant domain and a pcDNA 3.4 VL vector carrying the mouse kappa constant domain, respectively [34,35], to be expressed in mouse IgG2a/κ form. Similarly, engineered H9-derived Abs were subcloned. DNA encoding the full-length HLA-A*02:01 (residues 25–298, GenBank accession #: BC019236) was purchased from SinoBiological (cat. # HG13263-CH, Korea), and the human β2-microglobulin (β2m) gene was prepared by DNA synthesis (Bioneer, Daejeon, Korea). To express the recombinant pMHC protein in the single-chain trimer (SCT) form [19,20], the open-reading frame of the target (CMVpp65₄₉₅₋₅₀₃) or off-target (HPVE7₁₁₋₁₉) peptide-GCGGS(G₄S)₂ linker-β2m-(G₄S)₄ linker-extracellular domain of the HLA-A*02:01 protein (residues 25–298) with Y108C mutation-GS-Avi tag(GLNDIFEAQKIEWHE)-GS-8 × His tag was subcloned in-frame downstream of a secretion signal peptide in the pcDNA3.4 vector to be expressed as the CMVpp65₄₉₅₋₅₀₃/HLA-A*02:01 or HPVE7₁₁₋₁₉/HLA-A*02:01 SCT protein (Supplementary Figure S1).

4.2. Expression and Purification of Abs and Proteins

Plasmids encoding the heavy chain and light chain of Abs were transiently co-transfected in pairs, at equivalent molar ratios, into cultured mammalian human embryonic kidney HEK293F cells in Freestyle 293F medium (Invitrogen, CA, USA, 12338018) following the standard protocol [34,35]. Culture supernatants were collected after 6 days by centrifugation and filtration (0.22 μm, polyethersulfone; Corning). Abs were purified from the culture supernatants using a CaptivA™ Protein A-agarose chromatographic column (Repligen, MA, USA) and were extensively dialyzed to achieve the final composition of phosphate-buffered saline (PBS; pH 7.4). Likewise, the plasmid encoding the pMHC SCT protein was transfected into HEK293F cells. The pMHC protein was purified from the culture supernatant using Ni-NTA resin (GE Healthcare, IL, USA). Protein concentrations were determined using a bicinchoninic acid kit (Thermo Fisher Scientific, Waltham, MA, USA). To prepare an Ab-screening antigen, the purified pMHC SCT proteins were biotinylated using a BirA500 kit (Avidity LLC, Colorado, USA) following the manufacturer's instructions [35].

4.3. Enzyme-Linked Immunosorbent Assay (ELISA)

Binding activity and specificity of Abs to the purified CMVpp65₄₉₅₋₅₀₃/HLA-A*02:01 SCT protein were determined by ELISA, as described previously [17].

4.4. Cell Cultures

HLA-A*02:01-expressing cell lines Malme-3M, MDA-MB-231, and HCT116 and an HLA-A*02:01-negative LoVo cell line were purchased from the Korean Cell Line Bank and maintained and cultured in an RPMI-1640 medium (HyClone, Busan, Korea) supplemented with 10% heat-inactivated fetal bovine serum (FBS) (HyClone, Busan, Korea), penicillin (100 U/mL), streptomycin (100 µg/mL), and amphotericin B (0.25 µg/mL; HyClone) [35,36]. All cell lines were maintained at 37 °C in a humidified 5% CO₂ incubator and routinely screened for *Mycoplasma* contamination (CellSafe, Yongin-si, Korea).

4.5. Flow Cytometry

To determine the expression levels of HLA-A*02:01, cells (2.0×10^5 cells/mL) were incubated for 30 min with a PE-conjugated mouse anti-HLA-A2 monoclonal Ab (cat. # sc-32236 PE, Santa Cruz Biotechnology, diluted 1:100). After washing with 1 mL ice-cold PBS, cells were analyzed on a FACSCalibur flow cytometer (Becton-Dickinson, Franklin Lakes, New Jersey, USA). All staining procedures were performed at 4 °C.

To detect pMHC on cell surfaces, cells (3.0×10^5 cells/mL) were pulsed with the vehicle, CMVpp65₄₉₅₋₅₀₃, or HPVE7₁₁₋₁₉ peptide at the indicated concentration for 3 h at 37 °C, washed with fluorescence-activated cell sorting (FACS) buffer (1% FBS in PBS, pH 7.4), and resuspended at 1.5×10^5 cells/sample. All staining procedures were performed at 4 °C. Cells were incubated for 1 h with the TCR-like Ab at the indicated concentration, washed with 1 mL FACS buffer, and incubated with an Alexa Fluor 647-conjugated goat anti-mouse IgG-specific F(ab')₂ polyclonal Ab (cat. # 115-606-008, Jackson ImmunoResearch, diluted 1:600) for 30 min. After washing with 1 mL ice-cold PBS, cells were analyzed on the FACSCalibur flow cytometer. Data were analyzed using FlowJo V10 software (Tree Star).

4.6. Affinity Maturation of Abs

The yeast strains and media compositions have been previously described in detail [34,35]. Library generation of Abs by complementarity-determining region (CDR) mutagenesis was performed in the scFab format involving a G₄S-based 63-amino-acid linker between VL and VH, using YSD technology as described previously [17]. The yeast library was screened using magnetically activated cell sorting (MACS) and an FACS Aria III instrument (BD Biosciences) against biotinylated CMVpp65₄₉₅₋₅₀₃/HLA-A*02:01 SCT protein (with a gradual decrease in concentration from 2 µM to 0.4 nM) in the presence of a 10-fold higher concentration of non-biotinylated HPVE7₁₁₋₁₉/HLA-A*02:01 SCT protein as a competitor, as specified in the text. In FACS, cell surface expression and antigen binding levels of the scFab library were monitored by indirect double immunofluorescence labeling of the CH1 C-terminal c-myc tag (anti-c-myc mouse Ab [9E10], diluted 1:100) with an Alexa 488-labeled goat anti-mouse IgG Ab (Invitrogen, diluted 1:600) and streptavidin-conjugated R-phycoerythrin (Invitrogen, diluted 1:600). Typically, the top 0.1–0.2% of target-binding cells were sorted. The final sorted yeast cells were plated on a selective medium, and individual clones were isolated and further analyzed. DNA from the screened yeast cells was recovered using a Zymoprep kit (Zymo Research, CA, USA) as previously described [34,35].

4.7. Biolayer Interferometry

Kinetic binding interactions of TCR-like Abs with CMVpp65₄₉₅₋₅₀₃/HLA-A*02:01 SCT protein were monitored at pH 7.4 using an Octet QKe System (ForteBio, California, USA), as described previously [17,35]. All data were globally fitted via the 1:1 Langmuir binding model, and association and dissociation rate constants were calculated using Octet Data Analysis Software, version 11.0 (ForteBio, Fremont, CA, USA).

5. Patents

Patents resulting from the work reported in this manuscript have been filed in the Republic of Korea (Application number: KR 10-2020-0138273) and PCT (application number: PCT/KR2020/017067).

Supplementary Materials: The following are available online at <https://www.mdpi.com/1422-0067/22/5/2349/s1>.

Author Contributions: Conceptualization, Y.-S.K. and S.-Y.L.; methodology, S.-Y.L. and J.-A.K.; validation, D.-H.K. and M.-J.S.; investigation, S.-Y.L., D.-H.K., M.-J.S., J.-A.K., and K.J.; writing—original draft preparation, S.-Y.L. and Y.-S.K.; writing—review and editing, K.J. and Y.-S.K.; supervision, Y.-S.K.; project administration, Y.-S.K.; funding acquisition, Y.-S.K. All authors have read and agreed to the published version of the manuscript.

Funding: This research was funded by Samsung Future Technology Center (grant number SRFC-MA1802-09).

Institutional Review Board Statement: Not applicable.

Informed Consent Statement: Not applicable.

Data Availability Statement: All data in this study are available within the article or from the authors on request.

Conflicts of Interest: Y.S.K. and S.Y.L. are listed as inventors on the patent application (KR 10-2020-0138273; PCT/KR2020/017067) related to the technology described in this work. The other authors declare no conflicts of interest. The funders had no role in the design of the study; in the collection, analyses, or interpretation of data; in the writing of the manuscript, or in the decision to publish the results.

References

1. Limaye, A.P.; Babu, T.M.; Boeckh, M. Progress and Challenges in the Prevention, Diagnosis, and Management of Cytomegalovirus Infection in Transplantation. *Clin. Microbiol. Rev.* **2021**, *34*. [[CrossRef](#)]
2. Cannon, M.J.; Schmid, D.S.; Hyde, T.B. Review of cytomegalovirus seroprevalence and demographic characteristics associated with infection. *Rev. Med. Virol.* **2010**, *20*, 202–213. [[CrossRef](#)]
3. Lérias, J.R.; Paraschoudi, G.; Silva, I.; Martins, J.; de Sousa, E.; Condeco, C.; Figueiredo, N.; Carvalho, C.; Dodoo, E.; Jager, E.; et al. Clinically Relevant Immune Responses against Cytomegalovirus: Implications for Precision Medicine. *Int. J. Mol. Sci.* **2019**, *20*, 1986. [[CrossRef](#)]
4. Van der Merwe, P.A.; Davis, S.J. Molecular interactions mediating T cell antigen recognition. *Annu. Rev. Immunol.* **2003**, *21*, 659–684. [[CrossRef](#)] [[PubMed](#)]
5. Sylwester, A.W.; Mitchell, B.L.; Edgar, J.B.; Taormina, C.; Pelte, C.; Ruchti, F.; Sleath, P.R.; Grabstein, K.H.; Hosken, N.A.; Kern, F.; et al. Broadly targeted human cytomegalovirus-specific CD4⁺ and CD8⁺ T cells dominate the memory compartments of exposed subjects. *J. Exp. Med.* **2005**, *202*, 673–685. [[CrossRef](#)] [[PubMed](#)]
6. Wills, M.R.; Carmichael, A.J.; Mynard, K.; Jin, X.; Weekes, M.P.; Plachter, B.; Sissons, J.G. The human cytotoxic T-lymphocyte (CTL) response to cytomegalovirus is dominated by structural protein pp65: Frequency, specificity, and T-cell receptor usage of pp65-specific CTL. *J. Virol.* **1996**, *70*, 7569–7579. [[CrossRef](#)]
7. Weekes, M.P.; Wills, M.R.; Mynard, K.; Carmichael, A.J.; Sissons, J.G. The memory cytotoxic T-lymphocyte (CTL) response to human cytomegalovirus infection contains individual peptide-specific CTL clones that have undergone extensive expansion in vivo. *J. Virol.* **1999**, *73*, 2099–2108. [[CrossRef](#)] [[PubMed](#)]
8. Reiser, J.B.; Legoux, F.; Machillot, P.; Debeaupuis, E.; Le Moullac-Vaydie, B.; Chouquet, A.; Saulquin, X.; Bonneville, M.; Housset, D. Crystallization and preliminary X-ray crystallographic characterization of a public CMV-specific TCR in complex with its cognate antigen. *Acta Cryst. Sect. F Struct. Biol. Cryst. Commun.* **2009**, *65*, 1157–1161. [[CrossRef](#)]
9. Bewarder, M.; Held, G.; Thurner, L.; Stilgenbauer, S.; Smola, S.; Preuss, K.D.; Carbon, G.; Bette, B.; Christofyllakis, K.; Bittenbring, J.T.; et al. Characterization of an HLA-restricted and human cytomegalovirus-specific antibody repertoire with therapeutic potential. *Cancer Immunol. Immunother.* **2020**, *69*, 1535–1548. [[CrossRef](#)]

10. Wagner, E.K.; Qerqez, A.N.; Stevens, C.A.; Nguyen, A.W.; Delidakis, G.; Maynard, J.A. Human cytomegalovirus-specific T-cell receptor engineered for high affinity and soluble expression using mammalian cell display. *J. Biol. Chem.* **2019**, *294*, 5790–5804. [[CrossRef](#)] [[PubMed](#)]
11. Hoydahl, L.S.; Frick, R.; Sandlie, I.; Loset, G.A. Targeting the MHC Ligandome by Use of TCR-Like Antibodies. *Antibodies* **2019**, *8*, 32. [[CrossRef](#)] [[PubMed](#)]
12. He, Q.; Liu, Z.; Liu, Z.; Lai, Y.; Zhou, X.; Weng, J. TCR-like antibodies in cancer immunotherapy. *J. Hematol. Oncol.* **2019**, *12*, 99. [[CrossRef](#)] [[PubMed](#)]
13. Makler, O.; Oved, K.; Netzer, N.; Wolf, D.; Reiter, Y. Direct visualization of the dynamics of antigen presentation in human cells infected with cytomegalovirus revealed by antibodies mimicking TCR specificity. *Eur. J. Immunol.* **2010**, *40*, 1552–1565. [[CrossRef](#)]
14. Lefranc, M.P.; Lefranc, G. Immunoglobulins or Antibodies: IMGT((R)) Bridging Genes, Structures and Functions. *Biomedicines* **2020**, *8*, 319. [[CrossRef](#)]
15. Dunbar, J.; Deane, C.M. ANARCI: Antigen receptor numbering and receptor classification. *Bioinformatics* **2016**, *32*, 298–300. [[CrossRef](#)] [[PubMed](#)]
16. Lefranc, M.P.; Giudicelli, V.; Duroux, P.; Jabado-Michaloud, J.; Folch, G.; Aouinti, S.; Carillon, E.; Duvergey, H.; Houles, A.; Paysan-Lafosse, T.; et al. IMGT(R), The international ImMunoGeneTics information system(R) 25 years on. *Nucleic Acid. Res.* **2015**, *43*. [[CrossRef](#)] [[PubMed](#)]
17. Kim, J.E.; Jung, K.; Kim, J.A.; Kim, S.H.; Park, H.S.; Kim, Y.S. Engineering of anti-human interleukin-4 receptor alpha antibodies with potent antagonistic activity. *Sci. Rep.* **2019**, *9*, 7772. [[CrossRef](#)] [[PubMed](#)]
18. Kim, J.E.; Lee, D.H.; Jung, K.; Kim, E.J.; Choi, Y.; Park, H.S.; Kim, Y.S. Engineering of Humanized Antibodies Against Human Interleukin 5 Receptor Alpha Subunit That Cause Potent Antibody-Dependent Cell-Mediated Cytotoxicity. *Front. Immunol.* **2021**, *11*, 593748. [[CrossRef](#)] [[PubMed](#)]
19. Truscott, S.M.; Lybarger, L.; Martinko, J.M.; Mitaksov, V.E.; Kranz, D.M.; Connolly, J.M.; Fremont, D.H.; Hansen, T.H. Disulfide bond engineering to trap peptides in the MHC class I binding groove. *J. Immunol.* **2007**, *178*, 6280–6289. [[CrossRef](#)]
20. Schmittnaegel, M.; Hoffmann, E.; Imhof-Jung, S.; Fischer, C.; Drabner, G.; Georges, G.; Klein, C.; Knoetgen, H. A New Class of Bifunctional Major Histocompatibility Class I Antibody Fusion Molecules to Redirect CD8 T Cells. *Mol. Cancer. Ther.* **2016**, *15*, 2130–2142. [[CrossRef](#)]
21. Schirle, M.; Keilholz, W.; Weber, B.; Gouttefangeas, C.; Dumrese, T.; Becker, H.D.; Stevanovic, S.; Rammensee, H.G. Identification of tumor-associated MHC class I ligands by a novel T cell-independent approach. *Eur. J. Immunol.* **2000**, *30*, 2216–2225. [[CrossRef](#)]
22. Li, Y.; Moysey, R.; Molloy, P.E.; Vuidepot, A.L.; Mahon, T.; Baston, E.; Dunn, S.; Liddy, N.; Jacob, J.; Jakobsen, B.K.; et al. Directed evolution of human T-cell receptors with picomolar affinities by phage display. *Nat. Biotechnol.* **2005**, *23*, 349–354. [[CrossRef](#)]
23. Manning, C.F.; Bundros, A.M.; Trimmer, J.S. Benefits and pitfalls of secondary antibodies: Why choosing the right secondary is of primary importance. *PLoS ONE* **2012**, *7*. [[CrossRef](#)]
24. Vidarsson, G.; Dekkers, G.; Rispens, T. IgG subclasses and allotypes: From structure to effector functions. *Front. Immunol.* **2014**, *5*, 520. [[CrossRef](#)]
25. Kim, N.; Nam, Y.S.; Im, K.I.; Lim, J.Y.; Jeon, Y.W.; Song, Y.; Lee, J.W.; Cho, S.G. Robust Production of Cytomegalovirus pp65-Specific T Cells Using a Fully Automated IFN-gamma Cytokine Capture System. *Transfus. Med. Hemother.* **2018**, *45*, 13–22. [[CrossRef](#)]
26. Akatsuka, Y. TCR-Like CAR-T Cells Targeting MHC-Bound Minor Histocompatibility Antigens. *Front. Immunol.* **2020**, *11*, 257. [[CrossRef](#)]
27. Lai, J.; Choo, J.A.L.; Tan, W.J.; Too, C.T.; Oo, M.Z.; Suter, M.A.; Mustafa, F.B.; Srinivasan, N.; Chan, C.E.Z.; Lim, A.G.X.; et al. TCR-like antibodies mediate complement and antibody-dependent cellular cytotoxicity against Epstein-Barr virus-transformed B lymphoblastoid cells expressing different HLA-A*02 microvariants. *Sci. Rep.* **2017**, *7*, 9923. [[CrossRef](#)] [[PubMed](#)]
28. Zhao, Q.; Ahmed, M.; Tassev, D.V.; Hasan, A.; Kuo, T.Y.; Guo, H.F.; O'Reilly, R.J.; Cheung, N.K. Affinity maturation of T-cell receptor-like antibodies for Wilms tumor 1 peptide greatly enhances therapeutic potential. *Leukemia* **2015**, *29*, 2238–2247. [[CrossRef](#)] [[PubMed](#)]
29. Lowe, D.B.; Bivens, C.K.; Mobley, A.S.; Herrera, C.E.; McCormick, A.L.; Wichner, T.; Sabnani, M.K.; Wood, L.M.; Weidanz, J.A. TCR-like antibody drug conjugates mediate killing of tumor cells with low peptide/HLA targets. *mAbs* **2017**, *9*, 603–614. [[CrossRef](#)]
30. Khan, N.; Cobbold, M.; Keenan, R.; Moss, P.A. Comparative analysis of CD8+ T cell responses against human cytomegalovirus proteins pp65 and immediate early 1 shows similarities in precursor frequency, oligoclonality, and phenotype. *J. Infect. Dis.* **2002**, *185*, 1025–1034. [[CrossRef](#)] [[PubMed](#)]
31. Gerna, G.; Kabanova, A.; Lilleri, D. Human Cytomegalovirus Cell Tropism and Host Cell Receptors. *Vaccines* **2019**, *7*, 70. [[CrossRef](#)] [[PubMed](#)]
32. Plachter, B.; Sinzger, C.; Jahn, G. Cell types involved in replication and distribution of human cytomegalovirus. *Adv. Virus Res.* **1996**, *46*, 195–261. [[CrossRef](#)] [[PubMed](#)]
33. Stern-Ginossar, N.; Weisburd, B.; Michalski, A.; Le, V.T.; Hein, M.Y.; Huang, S.X.; Ma, M.; Shen, B.; Qian, S.B.; Hengel, H.; et al. Decoding human cytomegalovirus. *Science* **2012**, *338*, 1088–1093. [[CrossRef](#)] [[PubMed](#)]

34. Shin, S.M.; Choi, D.K.; Jung, K.; Bae, J.; Kim, J.S.; Park, S.W.; Song, K.H.; Kim, Y.S. Antibody targeting intracellular oncogenic Ras mutants exerts anti-tumour effects after systemic administration. *Nat. Commun.* **2017**, *8*, 15090. [[CrossRef](#)] [[PubMed](#)]
35. Shin, S.M.; Kim, J.S.; Park, S.W.; Jun, S.Y.; Kweon, H.J.; Choi, D.K.; Lee, D.; Cho, Y.B.; Kim, Y.S. Direct targeting of oncogenic RAS mutants with a tumor-specific cytosol-penetrating antibody inhibits RAS mutant-driven tumor growth. *Sci. Adv.* **2020**, *6*. [[CrossRef](#)] [[PubMed](#)]
36. Jung, K.; Kim, J.A.; Kim, Y.J.; Lee, H.W.; Kim, C.H.; Haam, S.; Kim, Y.S. A Neuropilin-1 Antagonist Exerts Antitumor Immunity by Inhibiting the Suppressive Function of Intratumoral Regulatory T Cells. *Cancer Immunol. Res.* **2020**, *8*, 46–56. [[CrossRef](#)] [[PubMed](#)]